Pressure-tuned quantum criticality in the antiferromagnetic Kondo semimetal $CeNi_{2-\delta}As_2$

Yongkang Luo[a,1], F. Ronning[a], N. Wakeham[a], Xin Lu[b], Tuson Park[c], Z.-A. Xu[d], and J. D. Thompson[a]

[a]Los Alamos National Laboratory, Los Alamos, NM 87545; [b]Center for Correlated Matter, Zhejiang University, Hangzhou 310058, China; [c]Department of Physics, Sungkyunkwan University, Suwon 440-746, South Korea; and [d]Department of Physics, Zhejiang University, Hangzhou 310027, China

Edited by Subir Sachdev, Harvard University, Cambridge, MA, and approved September 23, 2015 (received for review May 15, 2015)

The easily tuned balance among competing interactions in Kondo-lattice metals allows access to a zero-temperature, continuous transition between magnetically ordered and disordered phases, a quantum-critical point (QCP). Indeed, these highly correlated electron materials are prototypes for discovering and exploring quantum-critical states. Theoretical models proposed to account for the strange thermodynamic and electrical transport properties that emerge around the QCP of a Kondo lattice assume the presence of an indefinitely large number of itinerant charge carriers. Here, we report a systematic transport and thermodynamic investigation of the Kondo-lattice system $CeNi_{2-\delta}As_2$ ($\delta \approx 0.28$) as its antiferromagnetic order is tuned by pressure and magnetic field to zero-temperature boundaries. These experiments show that the very small but finite carrier density of $\sim 0.032\ e^-$/formular unit in $CeNi_{2-\delta}As_2$ leads to unexpected transport signatures of quantum criticality and the delayed development of a fully coherent Kondo-lattice state with decreasing temperature. The small carrier density and associated semimetallicity of this Kondo-lattice material favor an unconventional, local-moment type of quantum criticality and raises the specter of the Nozières exhaustion idea that an insufficient number of conduction-electron spins to separately screen local moments requires collective Kondo screening.

Kondo effect | quantum criticality | heavy Fermion | Nozières exhaustion | anomalous Hall effect

During the past decade or so, particular interest in Kondo-lattice systems has focused on those in which a moderate hybridization (J_{fc}) between magnetic f electrons and a sea of itinerant charge carriers allows their tuning by a nonthermal control parameter to a quantum-critical point (QCP) where non-Fermi-liquid (NFL) signatures appear in transport and thermodynamic properties (1). Although several models of quantum criticality have been proposed to account for various NFL properties (2, 3), a common assumption of these models is that the material is metallic. In these metals, the magnetic order that is tuned toward zero temperature is either of a local-moment type derived from Ruderman–Kittel–Kasuya–Yosida (RKKY) interactions when J_{fc} is relatively weak or a spin-density-wave (SDW) instability of a large Fermi surface to which the delocalized 4f state contributes when J_{fc} is stronger. An interesting question is what might be expected in a system with a very low carrier density and, additionally, how the low carrier density might influence the signatures of quantum criticality. A related issue is the nature of the magnetism that is being tuned in such a system. A low carrier density implies a dearth of conduction electrons and, consequently, a small Fermi wave vector. Under these circumstances SDW order is unlikely (but not impossible in principle); however, because the RKKY interaction depends on electrons near as well as deeper inside the Fermi sea (4), RKKY-mediated order is more favorable. Additionally, the cross-over from a low-temperature Fermi-liquid (FL) state to high-temperature local-moment state in a Kondo lattice can be slowed in the low carrier density limit, i.e., so-called protracted Kondo screening (5–7). New materials with tunable long-range magnetism and low carrier density are, therefore, of some interest.

At room temperature, $CeNi_{2-\delta}As_2$ ($\delta \approx 0.28$) crystallizes in the well-known $ThCr_2Si_2$-type structure (I4/mmm, no. 139) but may undergo a very weak orthorhombic distortion at low temperature (8). Well below this possible orthorhombic distortion, Ce moments order antiferromagnetically at $T_N \approx 5$ K (Fig. S1*A*) (8, 9), with the **c** axis being the magnetic easy axis. In the presence of an external magnetic field $\mathbf{B} \parallel$ c, the ordered Ce moments undergo a weakly first-order spin–flop transition from an antiferromagnetic (AFM) ground state to a polarized paramagnetic state. A magnetic structure was proposed in ref. 8 but remains to be confirmed; nevertheless, the existence of a spin–flop transition below T_N suggests that the order is of a local-moment type, which is also consistent with a modest zero-temperature Sommerfeld coefficient of 65 $mJ/mol \cdot K^2$ estimated by extrapolating the specific heat divided by temperature from above T_N (8). The magnetic entropy below T_N of $\sim 0.6R \ln 2$ indicates magnetic order in a crystalline electric field (CEF) doublet ground state and some f-c hybridization. Herein, we report the effects of hydrostatic pressure and applied magnetic field on the transport and thermodynamic properties of $CeNi_{2-\delta}As_2$. At atmospheric pressure, a pronounced anomalous Hall effect (AHE) scales well to a magnetization anomaly at the spin–flop, and it provides a useful means to track the pressure dependence of magnetic order at low temperatures, whereas the normal Hall coefficient confirms a low carrier density in $CeNi_{2-\delta}As_2$. The AFM order is suppressed gradually under pressure and vanishes at $p_c = 2.7$ GPa, above which an FL-like T^2 resistivity develops. We discuss the possibility of a pressure-driven QCP in this low carrier density Kondo lattice and its relation to a field-induced $T = 0$ boundary at $B_c = 2.8$ T under atmospheric pressure.

Significance

An unconventional quantum-critical point involves a critical destruction of the Kondo entanglement and a reconstruction of Fermi surface topology. A description of such quantum criticality requires a broader experimental basis and a theoretical model that includes critical fermionic degrees of freedom. We provide a rare example of peculiar quantum-critical behavior in the low carrier density limit. Most significantly, the similarity between our $CeNi_{2-\delta}As_2$ and the well-known quantum-critical Kondo-lattice system $CeCu_{6-x}Au_x$ indicates that a condition favorable for the unconventional quantum criticality is a "small" Fermi volume which disfavors the conventional Hertz–Millis-type spin-density-wave criticality. This insight provides new guidance for where new examples of unconventional quantum criticality could be found.

Author contributions: Y.L. and J.D.T. designed research; Y.L., F.R., and N.W. performed research; Y.L., X.L., T.P., and Z.-A.X. contributed new reagents/analytic tools; Y.L., F.R., and J.D.T. analyzed data; and Y.L., F.R., and J.D.T. wrote the paper.

The authors declare no conflict of interest.

This article is a PNAS Direct Submission.

[1]To whom correspondence should be addressed. Email: mpzslyk@gmail.com.

This article contains supporting information online at www.pnas.org/lookup/suppl/doi:10.1073/pnas.1509581112/-/DCSupplemental.

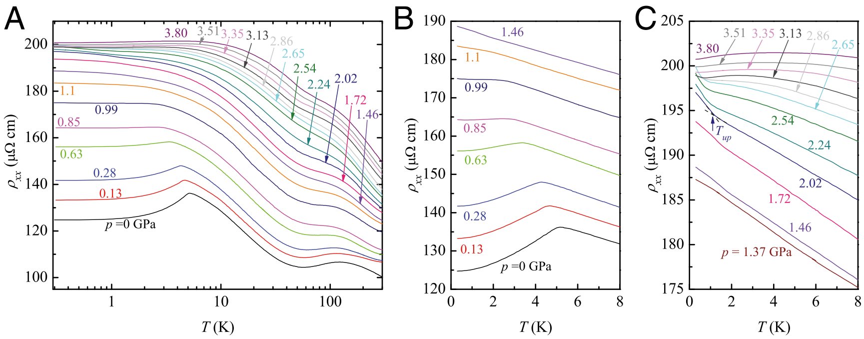

Fig. 1. Temperature dependence of the in-plane resistivity of $CeNi_{2-\delta}As_2$ under various pressures. (*A*) Data over the full temperature range. (*B* and *C*) Enlarged plots of $\rho_{xx}(T)$ below 8 K.

Results

The temperature-dependent resistivity $\rho_{xx}(T)$ of $CeNi_{2-\delta}As_2$ under various pressures is plotted in Fig. 1*A*. At ambient pressure, the large $\rho_{xx}(T)$ increases slowly with decreasing T, typical of semimetallic behavior, and there is a broad hump centered around 110 K. Such a broad hump in resistivity is ascribed to Kondo scattering on excited CEF levels. Below 50 K, $\rho_{xx}(T)$ increases approximately logarithmically with decreasing T, characteristic of Kondo scattering in the CEF doublet ground state. $\rho_{xx}(T)$ develops a sharp peak at $T_N = 5.1$ K, indicative of the reduction of spin scattering due to the formation of long-range order of Ce moments. As a function of pressure, five prominent tendencies are apparent. (*i*) Overall, the magnitude of resistivity increases with pressure, except for a narrow pressure range around 3 GPa and at very low temperatures, isobaric curves do not cross. This is not typical of the pressure response of Ce-based Kondo-lattice metals. (*ii*) The hump due to CEF splitting tends to be smeared but its position changes only slightly. (*iii*) The sharp peak at T_N is suppressed by pressure and is hardly observable when p exceeds 1.1 GPa (Fig. 1*B*). (*iv*) With further increasing pressure, an "inflection" appears below 2 K and $\rho_{xx}(T)$ turns up (Fig. 1*C*), signaling a further decrease in carrier concentration and/or an increase in scattering rate. Note that the evolution from peak to upturn seems continuous. Hall effect and ac heat capacity measurements, discussed below, indicate that in this pressure region Ce moments still order antiferromagnetically at low temperature. (*v*) For even higher pressure, the upturn in $\rho_{xx}(T)$ is absent and FL-like behavior with $\rho_{xx}(T) = \rho_0 + \Delta\rho = \rho_0 + AT^2$ is observed below a resistivity maximum at T_{coh} and typical of coherence in a Kondo lattice (data shown in Fig. 2*B*, *Inset* and Fig. S2). The fitted A coefficient for $P = 3.80$ GPa is 0.302 $\mu\Omega \cdot \mathrm{cm/K^2}$. From the Kadowaki–Woods ratio for a Kramers doublet ground state (10, 11), this A coefficient implies a Sommerfeld coefficient $\gamma = 170$ mJ/(mol $\cdot$ K^2), a value nearly three times that at ambient pressure [$\sim$ 65 mJ/(mol $\cdot$ K^2)] (8). We also point out that the smaller cell volume, isostructural analog $CeNi_2P_2$, is an intermediate valence compound (9). Our hydrostatic pressure experiment on $CeNi_{2-\delta}As_2$ is qualitatively consistent with a chemical pressure effect induced by P/As doping (12).

Fig. 2 *A* and *B* summarizes the effect of pressure on the field-dependent Hall resistivity $\rho_{yx}(B)$ at $T = 0.3$ K. The exchange interaction among Ce moments serves as an "effective internal field" that produces an AHE in addition to the normal Hall effect induced by a Lorentz force. For example, in Fig. 2*C* we show $\rho_{yx}(B)$ at $T = 2$ K under ambient pressure. The step-like increase in $\rho_{yx}(B)$ near $B = 2.55$ T is reminiscent of the spin–flop transition (8) observed in isothermal magnetization $M_c(B)$ plotted in Fig. 2*C*, *Inset*. Indeed, the $\rho_{yx}(B)$ curve can be well fit to the relation (13, 14)

$$\rho_{yx}(B) = R_H B + R_S \mu_0 M_c(B), \qquad [1]$$

in which R_H is the normal Hall coefficient and the second term characterizes the AHE contribution. The best fit leads to $R_H = -1.58 \times 10^{-8}$ m^3/C, and $R_S = 2.8 \times 10^{-6}$ m^3/C. The critical field B_c for the spin–flop transition can therefore be defined from the peak in $d\rho_{yx}/dB$ as depicted in Fig. 2*D*. Obviously, B_c moves to

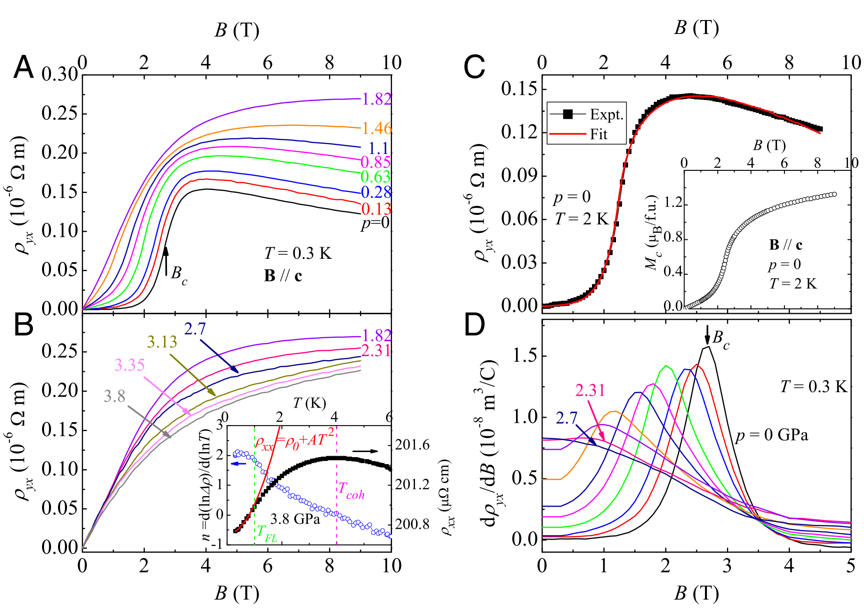

Fig. 2. Pressure-dependent Hall effect measurements on $CeNi_{2-\delta}As_2$. (*A* and *B*) Hall resistivity ρ_{yx} as a function of magnetic field at $T = 0.3$ K. (*C*) Fit of $\rho_{yx}(B)$ to Eq. **1**. (*Inset*) Plot of isothermal magnetization at $T = 2$ K with $\mathbf{B} \parallel c$. (*D*) The derivative of $\rho_{yx}(B)$. The peak in $d\rho_{yx}/dB$ defines the critical field of a spin–flop transition. (*B*, *Inset*) Local exponent $n = d(\ln \Delta\rho)/d(\ln T)$ (*Left*) and ρ_{xx} (*Right*) as functions of T for $P = 3.8$ GPa; T_{FL} and T_{coh} are defined as the temperatures where $n = 1.8$ and 0, respectively.

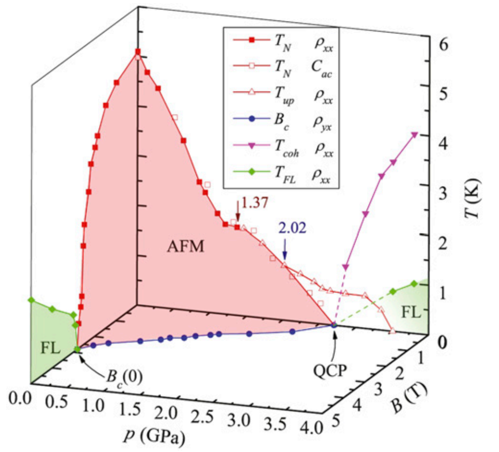

Fig. 3. *B-p-T* phase diagram of $CeNi_{2-\delta}As_2$. For clarity, we plot $B_c(p)$ in the $T = 0$ plane instead of the $T = 0.3$ K plane where measurements were made.

lower fields as p increases and terminates near 2.7 GPa as shown in Fig. 3. Taking a single band approximation for simplicity (which is also the upper bound of a multiband interpretation), the large magnitude of R_H corresponds to a low carrier density $n_c = 3.94 \times 10^{20}$ cm^{-3}, i.e., there are only $\sim$ 0.032 conduction electrons per formula unit, which corroborates the semimetallicity of $CeNi_{2-\delta}As_2$. The reason for such a low carrier density in $CeNi_{2-\delta}As_2$ is still unclear, but it is possible that Ni deficiency (8, 9) has shifted the Fermi level, leaving only a few carriers in the bottom of the renormalized conduction band. At pressures close to and well above 2.7 GPa, the transverse Hall resistivity remains nonlinear in field, reflecting the sum of skew scattering due to strong paramagnetism of Ce moments and a contribution from the normal Hall effect.

A global *B-p-T* phase diagram is plotted in Fig. 3. The field dependence of T_N at ambient pressure (on the *B-T* plane) is derived from combinations of $\rho_{xx}(T)$ at fixed B and $\rho_{ij}(B)$ at fixed T, whereas $T_N(p)$ is determined from $\rho_{xx}(T)$ and ac heat capacity measurements discussed below. The *B-p* boundary is defined from the pressure dependence of $d\rho_{yx}/dB$. At the zero-pressure critical field, $B_c(0) = 2.8$ T, the T-linear specific heat is a maximum [γ_0 = 657 mJ/(mol$\cdot$ K^2), as shown in Fig. 4*A*] and $\rho_{xx}(T)$ increases as $T^{1.53}$, indicative of a state similar to that found at field-tuned quantum criticality in metamagnetic systems (15–18). Fig. S3 provides more details. The $B_c(p)$ line at 0.3 K is continuous and terminates in zero field at p_c = 2.7 GPa, at which point $T_{coh}(p)$ and $T_{FL}(p)$, defined by data such as plotted in Fig. 2*B*, *Inset*, approach the $T = 0$ (0.3 K) plane. Combined with the recovery of FL-like behavior and the enhancement of quasi-particle effective mass, p_c defines a zero-field magnetic QCP. The question is, however, what is the nature of the two quantum criticalities, one in zero pressure at 2.8 T and the other in zero field at 2.7 GPa?

The presence of a spin–flop transition and the high magnetic anisotropy (8) at atmospheric pressure suggest that the magnetic order is of a local-moment type. On the other hand, this spin–flop transition, driven by a magnetic field, lacks spontaneous time-reversal symmetry breaking at the critical field: before the system reaches an intrinsic paramagnetic state, the moments already have been polarized (Fig. 4*A*). And, moreover, considering the weakly first-order nature of this field-induced spin–flop transition even at the low temperature of 0.3 K (Fig. S1*C*), B_c = 2.8 T is probably very close to a QCP.

In the absence of magnetic field, the pressure-induced quantum-phase transition at $p_c = 2.7$ GPa should be a second-order QCP. To further address this, we show ac heat capacity data (C_{ac}/T) in Fig. 4*B*. It is clearly seen that the λ-shaped peak corresponding to the AFM transition is gradually suppressed by pressure, and becomes undetectable at 2.72 GPa. We also note that C_{ac}/T at this pressure roughly obeys a $-\log T$ law at low temperature, strongly demonstrating an NFL behavior with divergent Sommerfeld coefficient that is in contrast with the one induced by field at B_c = 2.8 T (Fig. 4*A* and Fig. S4).

Discussion

The disparity between B- and p-induced quantum criticalities is reminiscent of $CeCu_{6-x}Au_x$ in which Au doping induces local-moment–like antiferromagnetism for $x > 0.1$ and non-SDW criticality, yet the field-induced critical behavior is characteristic of a 3D SDW QCP (19). In this regard, it is interesting that the nominally isoelectronic Au substitution for Cu results in a large reduction in carrier concentration, with n_c = − 0.73/formular unit (f.u.) for x = 0 and + 0.061/f.u. for x = 0.2, which is accompanied by a nearly fivefold increase in the low-temperature resistivity (20, 21). This change is not due to the emergence of AFM (20). An apparent dichotomy in the nature of the $T = 0$ boundaries as a function of doping (or pressure) versus that of field in $CeCu_{6-x}Au_x$ is found as well in $CeNi_{2-\delta}As_2$.

On the $B_c(p)$ line connecting B_c and p_c, there is a slight bump beginning at 1.37 GPa where a bump also appears on the line of $T_N(p)$. This pressure also coincides with a change in the resistive signature for magnetic order (Fig. 1 *B* and *C*) where at 1.37 GPa $\rho_{xx}(T)$ turns up through an inflection at T_{up} as it does in $CeCu_{5.8}Au_{0.2}$ (19). In the case of $CeCu_{5.8}Au_{0.2}$, an upturn in resistivity at the AFM transition was attributed to current flow with a component along the ordering wave vector **Q**, whereas the resistivity turns down below T_N when current flow is perpendicular to **Q** (21, 22). This provides a possible explanation for the pressure-induced evolution of the resistive signature for AFM in $CeNi_{2-\delta}As_2$, namely that

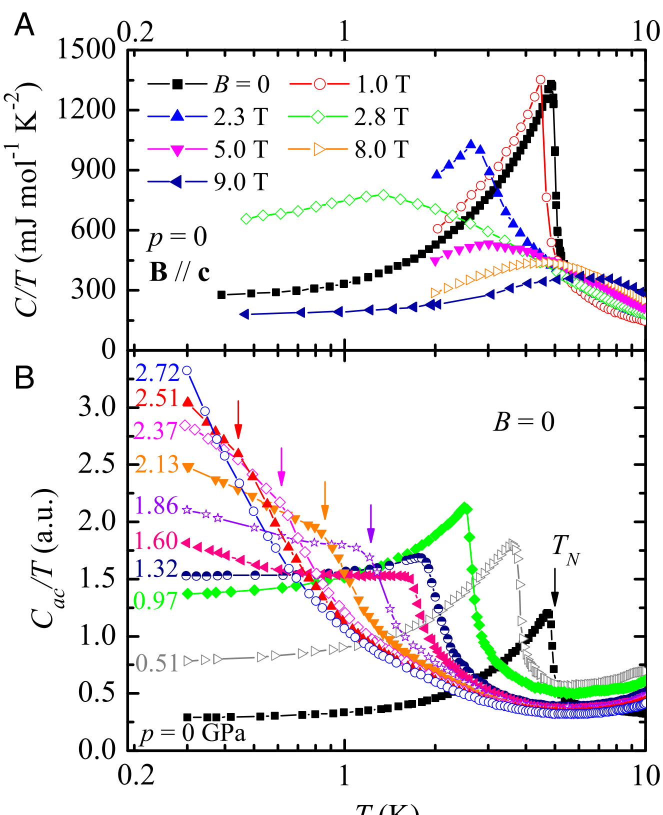

Fig. 4. (*A*) Atmospheric pressure specific heat of $CeNi_{2-\delta}As_2$ under various magnetic fields, with **B** ∥ c. (*B*) Temperature-dependent ac heat capacity under pressure; the arrows mark the positions of the AFM transitions.

a modest pressure induces a change in ordering wave vector for $p > 1.37$ GPa. By measuring magnetoresistivity in the configurations of $\mathbf{B} \parallel$ c and $\mathbf{B} \parallel$ ab (Fig. S5), we indeed find evidence for a magnetic order change from the **c** axis being the easy axis at low pressures to the **ab** plane being an easy plane at moderate pressures. Whether **Q** also changes simultaneously with pressure needs to be clarified in the future by microscopic techniques. This signature for AFM order persists to 2.02 GPa, above which $\rho_{xx}(T)$ evolves smoothly from above to below T_{up} (Fig. 1*C*). Fig. S2*A* provides a closer look of resistivity upturn in this pressure region. An extrapolation of $T_{up}(p)$ for $p \leq 2.02$ GPa to $T = 0$ intersects the pressure axis at p_c (Fig. 3), providing additional evidence for a pressure-tuned QCP at p_c. Nevertheless, above 2.02 GPa, $T_{up}(p)$ deviates from this extrapolation and forms an extra dome ranging from 2.02 to 3.51 GPa that we interpret to be a consequence of the low carrier concentration (see below). In this pressure range $T_{up}(p)$ is not a thermodynamic phase boundary.

Pressure, in general, promotes *f-c* hybridization in Ce-Kondo lattices and eventually suppresses AFM order as Kondo compensation of Ce moments begins to dominate. In $CeNi_{2-\delta}As_2$, pressure also appears to reduce the low carrier density even further, as witnessed by an overall increase in $\rho_{xx}(T,p)$ and the variation in $\rho_{yx}(B,p)$, and this counters the tendency for stronger hybridization by decreasing the Kondo-impurity temperature scale and, even more dramatically, the Kondo-lattice temperature scale below which a heavy Fermi liquid develops (23). A result of this protracted Kondo screening, which is related to the Nozières exhaustion idea that insufficient conduction states are available to screen all of the moments in a Kondo lattice (24), is the stabilization of RKKY-driven AFM order (23), which could include a change in ordering wave vector and provide a reasonable interpretation of the origin of a bump in $T_N(p)$ and $B_c(p)$ lines near 1.37 GPa. This concept of protracted screening also provides an appropriate explanation for the deviation of $T_{up}(p)$ from an extrapolation above 2.02 GPa. In this pressure regime, $T_{up}(p)$ reflects the temperature below which already strong scattering in the incoherent Kondo lattice is enhanced by the proliferation of magnetic fluctuations emerging from the projected QCP at p_c established by specific heat measurements. The evolution of conventional resistive signatures of quantum criticality is masked by this scattering. At pressures sufficiently above p_c, signatures of a coherent Kondo lattice (T_{coh} and T_{FL}) begin to appear, signaling that Kondo hybridization finally has overcome the counter tendency due to a reduced carrier density.

We cannot discount the possible role of Ni deficiencies and the associated disorder-induced Griffiths-phase singularities, but clearly Kondo physics in a low carrier system is primarily responsible for the *B-p-T* phase diagram of $CeNi_{2-\delta}As_2$. We note that the specific heat anomaly at T_N is quite sharp (Fig. 4*A*), demonstrating a well-defined second-order phase transition, and that the deficiencies reside in the Ni–As conduction layer whereas the Ce sublattice is free of deficiency. Assuming a spherical Fermi surface topology for simplicity and using the carrier density $n_c = 3.94 \times 10^{20}$ cm^{-3}, residual resistivity $\rho_0 = 125$ $\mu\Omega$ cm, and Sommerfeld coefficient $\gamma = 65$ mJ/mol$\cdot$K^2 at atmospheric pressure, we estimate a Fermi wave vector $k_F = 0.227$ Å^{-1}, effective mass $m^* = 55\ m_0$, and mean-free path $l = 189$ Å. Although this mean-free path is shorter than in very clean heavy-Fermion compounds, it is much longer than the average separation between Ni-site vacancies ($2a \approx 8$ Å), suggesting that potential scattering by Ni deficiencies does not dominate the magnitude of the resistivity. In $CeNi_{2-\delta}As_2$, the RKKY-driven AFM order of Ce moments, partially compensated by protracted Kondo screening, can be tuned by field or pressure to zero-temperature boundaries. Complications of competing pressure-enhanced hybridization and reduced carrier concentration prevent identification of the precise nature of criticality at p_c. Nonetheless, the emergence of a signature for Kondo coherence from p_c and a $-\log T$ dependence of C_{ac}/T at p_c suggest a condition unfavorable to SDW criticality but consistent with a local-moment type of criticality (2, 3, 12). A measure of the Fermi surface evolution around p_c would be instructive.

Conclusion

To summarize, we have mapped out the global *B-p-T* phase diagram of the low carrier density AFM Kondo semimetal $CeNi_{2-\delta}As_2$ by transport and thermodynamic measurements. There are two $T = 0$ boundaries on this phase diagram, one induced by magnetic field and the other by pressure. The field-tuned boundary at $B_c = 2.8$ T, of weakly first-order nature, is probably very close to a $T = 0$ QCP of some type, whereas the pressure-tuned QCP at $p_c = 2.7$ GPa is accompanied by the development of Kondo coherence and divergent quasi-particle effective mass, and thus points to an unconventional QCP. The competition between low carrier density and pressure-enhanced Kondo hybridization plays an important role in the evolution of Néel order and signatures of criticality. $CeNi_{2-\delta}As_2$ provides an interesting paradigm of quantum criticality in the limit of low carrier density, evoking the need for a reexamination of the Nozières exhaustion problem and its possible consequences for quantum criticality.

PHYSICS

Materials and Methods

Millimeter-sized single crystals of $ThCr_2Si_2$-type $CeNi_{2-\delta}As_2$ were synthesized by a NaAs-flux method as described elsewhere (8). Rietveld analysis of X-ray spectra obtained on powdered single crystals confirms the I4/*mmm* structure and indicates that the Ni site occupancy is 0.856, close to the result of 0.86 obtained from energy-dispersive X-ray microanalysis measurements. Electrical transport measurements were made on two samples (denoted by **S1** and **S2**) as functions of pressure and field. **S1** was pressurized in an indenter-type cell up to 3.80 GPa in the configuration $\mathbf{B} \parallel$ c, whereas measurements on **S2** were performed in a piston-clamp cell up to 2.65 GPa with **B** perpendicular to **c**. Data on both samples agree quantitatively. Ohmic contacts were made in a Hall-bar geometry, and in-plane electrical resistivity (ρ_{xx}) and Hall resistivity (ρ_{yx}, **S1** only) down to 0.3 K were measured by an LR-700 ac resistance bridge. Heat capacity of $CeNi_{2-\delta}As_2$ under pressure (up to 2.72 GPa) was measured by an ac calorimetric method. For all these measurements, Daphne oil 7474 was used as a pressure-transmitting medium, and the pressure was determined by measuring the superconducting transition of Pb.

ACKNOWLEDGMENTS. We thank E. D. Bauer, R. Movshovich, and M. Janoschek for helpful discussions. Work at Los Alamos was performed under the auspices of the US Department of Energy, Division of Materials Sciences and Engineering. Y.L. acknowledges a Director's Postdoctoral Fellowship supported through the Los Alamos Laboratory Directed Research and Development (LDRD) program. Work at Zhejiang University was supported by the National Science Foundation of China (Grants 11374257 and 11190023) and the Fundamental Research Funds for the Central Universities. T.P. acknowledges support from a National Research Foundation (NRF) grant funded by the Ministry of Science, Information and Communications Technology (ICT) and Future Planning of Korea (no. 2012R1A3A2048816).

1. Doniach S (1977) The Kondo lattice and weak antiferromagnetism. *Physica B+C* 91:231–234.
2. Löhneysen Hv, Rosch A, Vojta M, Wolfle P (2007) Fermi-liquid instabilities at magnetic quantum phase transitions. *Rev Mod Phys* 79(3):1015–1075.
3. Gegenwart P, Si Q, Steglich F (2008) Quantum criticality in heavy-fermion metals. *Nat Phys* 4(3):186–197.
4. Neto AHC, Jones BA (2000) Non-Fermi-liquid behavior in U and Ce alloys: Criticality, disorder, dissipation, and Griffiths-McCoy singularities. *Phys Rev B* 62(22):14975–15011.
5. Tahvildar-Zadeh AN, Jarrell M, Freericks JK (1997) Protracted screening in the periodic Anderson model. *Phys Rev B* 55(6):R3332–R3335.
6. Sarrao JL, et al. (1999) Physical properties of $YbXCu_4$ (*X*=Ag, Au, Cd, Mg, Tl, and Zn) compounds. *Phys Rev B* 59(10):6855–6866.
7. Lawrence JM, et al. (2001) Slow crossover in $YbXCu_4$ (*X*=Ag, Cd, In, Mg, Tl, Zn) intermediate-valence compounds. *Phys Rev B* 63(5):054427.
8. Luo Y, et al. (2012) Magnetism and crystalline electric field effect in $ThCr_2Si_2$-type $CeNi_2As_2$. *Phys Rev B* 86(24):245130.
9. Suzuki H, Abe H, Kitazawa H, Schmitt D (2001) Magnetic properties and resistivity of ternary compounds $CeNi_2X_2$ (X=Sb, As, P). *J Alloys Compd* 323-324:520–523.
10. Kadowaki K, Woods SB (1986) Universal relationship of the resistivity and specific heat in heavy-Fermion compounds. *Solid State Commun* 58(8):507–509.

11. Tsujii N, Kontani H, Yoshimura K (2005) Universality in heavy fermion systems with general degeneracy. *Phys Rev Lett* 94(5):057201.
12. Luo Y, et al. (2014) Heavy-fermion quantum criticality and destruction of the Kondo effect in a nickel oxypnictide. *Nat Mater* 13(8):777–781.
13. Smith AW, Sears RW (1929) The Hall effect in Permalloy. *Phys Rev* 34(11):1466–1473.
14. Hurd C (1972) *The Hall Effect in Metals and Alloys* (Plenum, New York), p 153.
15. Grigera SA, et al. (2001) Magnetic field-tuned quantum criticality in the metallic ruthenate $Sr_3Ru_2O_7$. *Science* 294(5541):329–332.
16. Balicas L, et al. (2005) Magnetic field-tuned quantum critical point in $CeAuSb_2$. *Phys Rev B* 72(6):064422.
17. Mun ED, Bud'ko SL, Kreyssig A, Canfield PC (2010) Tuning low-temperature physical properties of $CeNiGe_3$ by magnetic field. *Phys Rev B* 82(5):054424.
18. Millis AJ, Schofield AJ, Lonzarich GG, Grigera SA (2002) Metamagnetic quantum criticality in metals. *Phys Rev Lett* 88(21):217204.
19. Löhneysen Hv, Pfleiderer C, Pietrus T, Stockert O, Will B (2001) Pressure versus magnetic-field tuning of a magnetic quantum phase transition. *Phys Rev B* 63(13): 134411.
20. Bartolf H, Pfleiderer C, Stockert O, Vojya M, Löhneysen Hv (2005) Hall effect across the quantum phase transition of $CeCu_{6-x}Au_x$. *Physica B* 359-361:86–88.
21. Löhneysen Hv, et al. (1998) Heavy-fermion systems at the magnetic-nonmagnetic quantum phase transition. *J Magn Magn Mater* 177-181:12–17.
22. Löhneysen Hv, et al. (1998) Magnetic order and transport in the heavy-fermion system $CeCu_{6-x}Au_x$. *Eur Phys J B* 5(3):447–455.
23. Pruschke T, Bulla R, Jarrell M (2000) Low-energy scale of the periodic Anderson model. *Phys Rev B* 61(19):12799–12809.
24. Nozières P (1998) Some comments on Kondo lattices and the Mott transition. *Eur Phys J B* 6(4):447–457.
25. Hertz JA (1976) Quantum critical phenomena. *Phys Rev B* 14(3):1165–1184.
26. Millis AJ (1993) Effect of a nonzero temperature on quantum critical points in itinerant fermion systems. *Phys Rev B Condens Matter* 48(10):7183–7196.
27. Stewart GR (2001) Non-Fermi-liquid behavior in *d*- and *f*-electron metals. *Rev Mod Phys* 73(4):797–855.
28. Custers J, et al. (2003) The break-up of heavy electrons at a quantum critical point. *Nature* 424(6948):524–527.